


ORIGINAL INNOVATION

Open Access



Extraction and evaluation of cable forces of a cable-stayed bridge based on amplitude and phase estimation method

Weiguo Wang¹, Xiaodong Song^{2,3*} , Yang Yu², Hongchen Chang⁴, Wenxin Yu² and Wen Xiong²

*Correspondence:
xdsong@seu.edu.cn

¹ School of Civil Engineering,
Southeast University,
Nanjing 211189, China

² School of Transportation,
Southeast University,
Nanjing 211189, China

³ Key Laboratory of Safety
and Risk Management
on Transport Infrastructures,
Ministry of Transport,
Nanjing 211189, China

⁴ Nanjing Urban Construction
Investment Holding (Group) Co.
Ltd., Nanjing 210009, China

Abstract

In order to identify the time-varying frequency and amplitude of structural vibration based on the bridge structural health monitoring data and obtain the cable force of cable-stayed bridges in real time, a spectrum analysis method based on amplitude and phase estimation (APES) was proposed in this study. The amplitude spectrum of the acceleration data is first calculated by the APES method, the real-time spectrogram of the cable is obtained by the sliding window method. Then the modal frequency and amplitude are automatically extracted from the real-time spectrum by using a frequency extrusion post-processing technique, which can be regarded as the average value of the instantaneous frequency and amplitude respectively. Next, the fundamental frequency of the cable is extracted by using an automatic identification method, and the performance of the proposed method is verified. Finally, real-time scoring of cable forces and structural condition assessment is achieved with consideration of the moderation index model as well as the material strength. The results show that the APES method can use shorter calculation samples than the traditional Fast Fourier Transform (FFT) to obtain higher resolution and more accurate amplitude, which provides a theoretical basis for the real-time identification of fundamental frequency based on short-term monitoring data. The frequency extrusion post-processing-algorithm can reduce the spectrum recognition delay and improve timeliness of the cable force evaluation. The time-varying cable force with an interval of 10s can be used to reflect the health status of the cable in time. The research results can provide technical support for the real-time extraction of cable force of long-span cable-stayed bridges, and can also provide an effective basis for component condition evaluation and bridge maintenance decision-making.

Keywords: Cable-stayed bridges, Frequency tracking, Structural health monitoring, Cable force evaluation, Frequency-squeezing postprocessing

1 Introduction

In recent years, large civil structures such as bridges, buildings, and dams have been equipped with Structural Health Monitoring Systems (Noel et al. 2017). As the intrinsic dynamic characteristic of the structure, frequency is one of the most important indicators in the evaluation of the service performance of the structure. For engineering

service structures, especially long-span bridges carrying live loads, they exhibit non-stationary and nonlinear dynamic characteristics. Therefore, the identification of time-varying frequency of structures has become one of the research hotspots. Baccigalupi and Liccardo (2016), Ni et al. (2018), Xin et al. (2021) used different methods such as empirical mode decomposition, variational mode decomposition and analytical mode decomposition to decompose the measured multi-component response into a limited number of intrinsic mode functions, and the Hilbert transform is used to identify the frequency, thereby realizing frequency identification based on the mode. Pai (2010) and Zhong and Pai (2021) proposed a sliding window tracking method and a conjugate pair decomposition method for frequency recognition after obtaining the intrinsic mode function, and explored the influence of the final effect of the Gibbs phenomenon. In addition, Cicone et al. (2016) mitigated the final effect and gained the ability to characterize the local features of the signal by mapping the intrinsic mode function in cartesian coordinate system to that in polar coordinates. Yang et al. (2016) proposed a method to identify time-varying cable forces based on a complexity tracking algorithm, where sensor optimization need to be considered. Hou et al. (2021) combined the advantages of variational mode decomposition and Hilbert transform together to recognize the time-varying cable force. Zhang et al. (2020) used synchronous compression transform method based on short-time Fourier transform to identify the instantaneous frequency of the cable. Synthesize all of above, for many time-varying cable force identification methods based on time-frequency analysis, the choice of time-frequency analysis algorithm is related to the robustness and accuracy of time-varying cable force identification. In the case of low signal-to-noise ratio, traditional time-frequency analysis algorithms have difficulty in extracting the ridge, so it cannot meet the accuracy requirements of online real-time frequency identification.

The cable force of a cable-stayed bridge is the core indicator to ensure the reasonable performance and safety status of the bridge structure during operation. Obtaining the time-varying cable force based on the monitored data measured by acceleration sensor can reflect the stress state and changing trend of the entire structure. Li et al. (2018) used Gaussian Mixture Model (GMM) to denote the cable tension ratio pattern, and the number of patterns representing model complexity was determined by Bayesian information criterion. Other parameters of GMM were estimated using the expected maximization algorithm under the maximum likelihood criterion based on the monitored cable tension. The vibration based cable tension estimation method requires complex calculations, especially when a comprehensive cable model is required. In order to avoid complex mathematical calculations, Zarbaf et al. (2018) proposes a simple new framework for cable tension estimation based on artificial neural networks. Ali et al. (2020) applied the first-order reliability method and Monte Carlo method to determine the reliability index of stay cables.

In this paper, the natural frequency and amplitude of cables are automatically extracted from the spectrum obtained by amplitude phase estimation, which has a higher resolution than the Fast Fourier Transform (FFT) method. Then, a post-processing technology is used to automatically extract the frequency and amplitude after concentrating the spectral lines. The time-varying fundamental frequency and the associated cable force time history is obtained. The detected cable forces of a cable-stayed bridge are evaluated

according to the interpolation of the moderate index model to realize the real-time assessment of the bridge service performance.

2 Spectrum identification based on amplitude and phase estimation

2.1 Background engineering

The double-tower double-cable-stayed bridge is chosen in this study, which has a main span of 510m. The span is arranged as 50m + 215m + 510m + 215m + 50m. The main beam of the bridge adopts a flat streamlined steel box girder, and the bridge width is 30m. The distance between the longitudinal diaphragms of the box girder along the bridge is 4.0m. The tower adopts reinforced concrete to separate the upper tower column inverted Y-shaped cable tower, with the height of 184.781m. The cable numbers are denoted as A1 ~ A16 and J1 ~ J16 respectively, wherein A8, A16, J8 and J16 upstream and downstream cables are installed with accelerometers for cable force monitoring. The general arrangement schematic diagram of the bridge is shown in Fig. 1.

2.2 Amplitude and phase estimation algorithms

Amplitude and phase estimation was first proposed by Li and Stoica (1996), which is a non-parametric adaptive filter bank method. The discrete one-dimensional time series $\{x(n)\}_{n=0}^{N-1}$, for the frequency of interest, can be decomposed into the sinusoidal term with amplitude $\alpha(\omega)$ and the sum of remaining term $\varepsilon_\omega(n)$ including sinusoidal components of other frequencies and all interference caused by random noise:

$$x(n) = \alpha(\omega)e^{j2\pi\omega n} + \varepsilon_\omega(n), n = 0, 1, \dots, N - 1 \tag{1}$$

where N is the length of computing frame.

Arrange N consecutive samples in an $M \times L$ Hankel matrix:

$$Y = [y_0 \ y_1 \ \dots \ y_{L-1}] = \begin{bmatrix} x(0) & x(1) & \dots & x(L-1) \\ x(1) & x(2) & \dots & x(L) \\ \vdots & \vdots & \ddots & \vdots \\ x(M-1) & x(M) & \dots & x(N-1) \end{bmatrix} \tag{2}$$

where $M \leq N/2$ is a user-defined parameter; and $L = N + 1 - M$.

In the interpretation of the matched filter bank in APES, the core is to design a data-dependent finite impulse response (FIR) filter $h(\omega) \in C^{M \times 1}$ that passes sine curves with

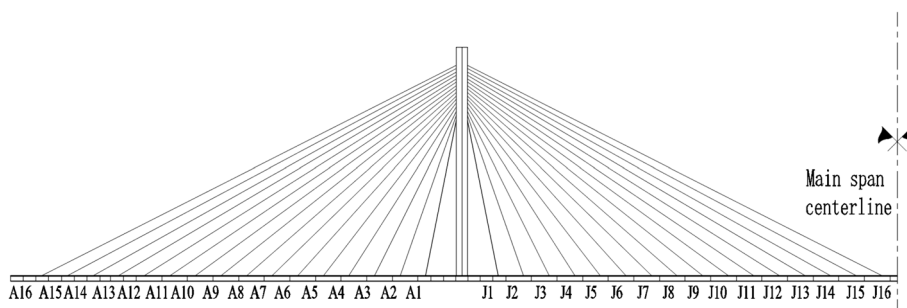


Fig. 1 Cable number of the cable-stayed bridge

frequency ω without distortion and suppresses sine curves of any other frequencies as much as possible:

$$\min_{\mathbf{h}(\omega), \alpha(\omega)} \sum_{l=0}^{L-1} \left| \mathbf{h}^H(\omega) \mathbf{y}_l - \alpha(\omega) e^{j2\pi\omega l} \right|^2 \quad \text{s.t.} \quad \mathbf{h}^H(\omega) \mathbf{f}_M(\omega) = 1 \quad (3)$$

thereinto

$$\mathbf{f}_M(\omega) = [1 \quad e^{j2\pi\omega} \quad \dots \quad e^{j2\pi\omega(M-1)}]^T \quad (4)$$

where $(\cdot)^H$ and $(\cdot)^T$ denotes the conjugate transpose and transpose of a vector or matrix respectively.

The closed-form solution of Eq. (3) can be expressed as:

$$\mathbf{h}(\omega) = \frac{\mathbf{Q}(\omega)^{-1} \mathbf{f}_M(\omega)}{\mathbf{f}_M^H(\omega) \mathbf{Q}(\omega)^{-1} \mathbf{f}_M(\omega)}, \quad (5)$$

$$\alpha(\omega) = \mathbf{h}^H(\omega) \mathbf{g}(\omega) = \frac{\mathbf{f}_M^H(\omega) \mathbf{Q}(\omega)^{-1} \mathbf{g}(\omega)}{\mathbf{f}_M^H(\omega) \mathbf{Q}(\omega)^{-1} \mathbf{f}_M(\omega)}, \quad (6)$$

where $\mathbf{g}(\omega)$ and $\mathbf{Q}(\omega)$ can be expressed as:

$$\mathbf{g}(\omega) = \frac{1}{L} \sum_{l=0}^{L-1} \mathbf{y}_l e^{-j2\pi\omega l} = \frac{1}{L} \mathbf{Y} \mathbf{f}_L^*(\omega), \quad (7)$$

$$\mathbf{Q}(\omega) = \frac{1}{L} \mathbf{Y} \mathbf{Y}^H - \mathbf{g}(\omega) \mathbf{g}^H(\omega) = \mathbf{R} - \mathbf{g}(\omega) \mathbf{g}^H(\omega) \quad (8)$$

where $(\cdot)^*$ denotes the conjugation of a vector or matrix.

2.3 Comparison between APES and FFT

The common method for identifying the natural frequency is using FFT to transform the acceleration time history to obtain the spectrum and detect the natural frequency based on the peak. However, this method has certain limitations when identifying cable forces. The frequency resolution of the FFT algorithm is determined by the length of the time window. Increasing the resolution requires increasing the length of the time window, which will increase the calculation time and the amount of data recorded, and reduce the efficiency. For the sampling frequency of the cable accelerometer on conventional long-span bridges, it often takes hundreds or even thousands of seconds of data to calculate the cable force value with acceptable accuracy, which is difficult to detect the instantaneous change of cable force in time and accurately, which is not conducive to the early warning of emergencies.

APES method has the following characteristics in the on-line analysis of monitoring signals: (1) compared with FFT, APES spectra are data-correlated, with narrower main lobes and lower side lobes, that is, higher (waveform) resolution; (2) The APES spectra can arbitrarily specify the calculation frequency accuracy and the calculation frequency interval, whereas in FFT, the calculation accuracy (without zero padding) and the

calculation interval are fixed at $1/T$ and $[0, F_s/2]$ respectively, where T is the sampling time duration, and F_s is the sampling frequency; (3) APES can obtain higher resolution and more accurate amplitude by utilizing a shorter computational frame length than FFT.

Taking the acceleration time history of A8 cable in the North Tower as an example, for the acceleration time history data with a sampling frequency of 20 Hz, the spectrogram obtained by APES and FFT is shown in Fig. 2. Figure 2a-c represent FFT spectrograms obtained from data with the time length of 120 s, 500 s, and 1000 s. Figure 2d represents spectrogram obtained from data with time duration of 120 s, and the calculated frequency vector range of 0–4 Hz is specified.

From the comparison of Fig. 2a and d, it can be seen that for the same number of sampling points, APES has a narrower main lobe and a lower side lobe, and the recognition accuracy is higher. The calculated frequency vector of APES is specified as $[0, 0.001, 0.002, \dots, 4]$ Hz, while the calculated frequency vector of FFT is $[0, 1/T, 2/T, \dots, 10]$ Hz, where T is taken for 120 s, 500 s, and 1000 s, respectively. As can be seen from Fig. 2a-d, the resolution ratio of the FFT method gradually increases with the increase of the sampling length T . Figure 2 also shows that the resolution ratio of the APES spectrum obtained with a sample length of 120 s, can compare favorably with that of FFT method with the sample length of 500 s and 1200 s.

According to the accuracy requirements of the cable force calculation, the frequency resolution is set as 0.001 Hz, and the corresponding time length of the acceleration time history should be 1000 s. In FFT calculations, in order to obtain accurate amplitude information, the calculated frame length needs to be set to at least 20,000 sample points so that

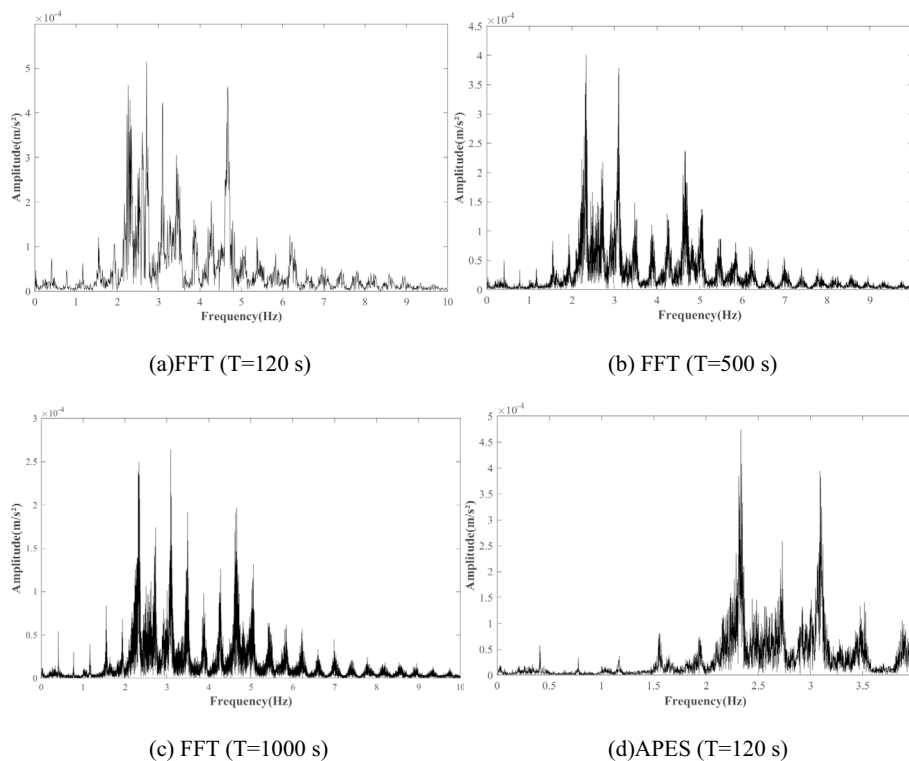


Fig. 2 Acceleration time-history spectrogram of the upstream side of A8 cable

the true frequency falls on its frequency grid. When the time duration of 500 s is used, the calculated frequency resolution of the FFT is 0.002 Hz, and the associated spectrogram misses the second frequency of 0.775 Hz, resulting in the abnormal display of the top of the second main lobe. It should be noted that the calculated frequency vector of the APES method is not limited by the length of the analyzed signal and can be arbitrarily specified, so the calculated frame length is not limited by the calculation accuracy requirements. Moreover, the calculation speed can be improved by specifying the calculation interval and reducing the meaningless calculation, and the frequency resolution can be arbitrarily specified. In summary, the APES method has good advantages in terms of real-time and calculation accuracy, and is suitable for the perception of time-varying frequency.

3 Automatic identification and extraction of fundamental frequency

3.1 Frequency squeezing post-processing technology

There has been a lot of researches on how to improve the readability of time-frequency analysis. Recently, some post-processing methods have been proposed, such as Reassignment Method (RM) and Synchronous Squeezing Transform (SST). RM reallocates the time-frequency coefficients of STFT on the time-frequency axis based on the centroid of the local energy distribution in the spectrum. SST is a post-processing method based on time-frequency analysis, whose main idea is to compress the spectrum in the frequency direction, making the analysis results more accurate and readable. Compared with RM, SST has higher computational efficiency and can better reconstruct the original signal. SST has been widely used in fields such as mechanical damage diagnosis, medical signal processing, and vibration signal processing, having achieved good results.

A frequency squeezing post-processing technique (FSP) was used (Yu and Dan 2022) in order to improve the TFR resolution of BRAPES. The main idea is to move equidistant spectral lines in the frequency direction, making their frequency non-uniform and having a higher density at the natural frequency, which can improve the resolution and accuracy of time-frequency analysis. FSP has wide applications in fields such as structural modal analysis. Throughout the entire processing, the amplitude remains unchanged to ensure its usability in time-frequency analysis. Although MSLM does not have the same good mathematical foundation and characteristics as RM and SST, it has demonstrated good time-frequency representation ability in practical applications.

In order to improve the time-frequency representation resolution of APES, frequency squeezing post-processing technology is used here (Yu and Dan 2022). This method shifts the equally spaced spectral lines in the frequency direction so that their frequencies become non-uniformly distributed and have a large density at the natural frequency. This method can improve the resolution and accuracy of time-frequency analysis, and is widely used in fields such as structural mode analysis. During the entire processing, the amplitude does not change, ensuring its usability in time-frequency analysis.

As a post-processing technology for concentrating spectral lines, FSP consists of three steps: (1) amplitude pretreatment, (2) frequency compression, and (3) amplitude recovery and zeroing.

First, the APES spectra $\alpha = [\alpha_1, \alpha_2, \dots, \alpha_K]^T$ were preprocessed by normalization and exponentiation:

$$\bar{\alpha}_i = (\alpha_i / \max(\alpha))^m, \quad i = 1, 2, \dots, K, \quad m > 1. \tag{9}$$

Then, consider the continuous $2P + 1$ spectral line $(\bar{\alpha}_{i-P}, \dots, \bar{\alpha}_i, \dots, \bar{\alpha}_{i+P})$ centered on frequency ω and replace the value of ω with the centroid of the spectrum in the direction of frequency to squeeze the evenly distributed lines:

$$\omega_i^{n+1} = \frac{\sum_{k=\max(1, i-P)}^{\min(i+P, K)} \omega_k^n \bar{\alpha}_k}{\sum_{k=\max(1, i-P)}^{\min(i+P, K)} \bar{\alpha}_k}, \quad i = 1, 2, \dots, K, \quad P \geq 1. \tag{10}$$

By iteratively executing Eq. (10), the original spectral lines will gradually concentrate near the location of the highest local peak. Here, the convergence criterion is set as the Euclidean distance between the n th frequency vector ω^n and the $(n + 1)$ th frequency vector ω^{n+1} should be less than the threshold δ_s , that is, $\|\omega^{n+1} - \omega^n\|_2 \leq K\delta_s$. At the same time, set the maximum number of steps for iterative calculation.

Finally, the original amplitude vector α is assigned to the compressed frequency vector $\hat{\omega}$ in subscript order, restoring the amplitude changed in step 1. At the same time, set the amplitude at both ends of the frequency vector $\hat{\omega}$ and at the edge of the cluster to zero to obtain a clearer representation of the results:

$$\hat{\alpha}_i = \begin{cases} 0, & i \in \Omega = \{1, K\} \cup \{(j, j + 1) | \hat{\omega}_{j+1} - \hat{\omega}_j > \delta_\omega\}, \\ \alpha_i, & i \in \{1, 2, \dots, K\} \setminus \Omega, \end{cases} \tag{11}$$

where δ_ω is the threshold used to judge the edge of the frequency clusters.

3.2 The influence of parameters on FSP algorithm

The analog signal is used as an example to analyze the influence of parameters.

$$sig = 1.42 \cos(2\pi \times 2.32t) + 1.07 \cos(2\pi \times 3.17t) + 0.89 \cos(2\pi \times 4.23t + \pi/4) + noise \sim \mathcal{N}(0, 0.02^2) \tag{12}$$

where $noise \sim \mathcal{N}(0, 0.02^2)$ represents Gaussian white noise with a standard deviation of 0.2. Assuming the sampling frequency is 100 Hz.

In the APES algorithm, the spectrogram obtained with finite impulse response filter lengths M of different sizes is shown in Fig. 3. The effect of sample length N on spectral

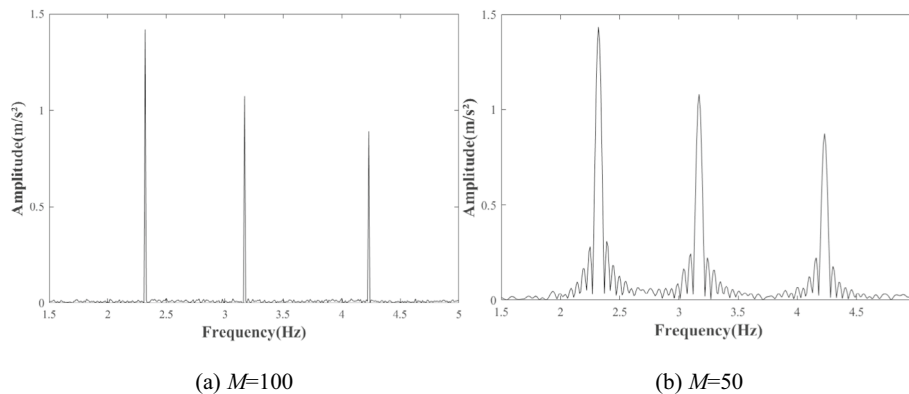


Fig. 3 APES spectrogram ($N = 2400$)

effect is similar to that of M . It can be seen that larger M can obtain good spectral effect, but the calculation time cost is significantly greater than that of smaller M .

As can be seen from Fig. 4a and b, the accuracy of the main lobe will improve with the increase of the power order m of the amplitude preprocessing in the FSP algorithm, but the image of the noisy side lobes will also be more obvious. Comparing Fig. 4a and c, changing the analysis step size of $2p + 1$ while squeezing the spectral line, due to the low signal-to-noise ratio, there will be some small noise side lobes in the spectral line, but with the increase of p , the noise side lobe will gradually converge with the main lobe, approach the main lobe, and be absorbed by the main lobe, which manifests as the value of the noise side lobe gradually disappearing.

The aggregation effect of the FSP post-processing technique on the spectrum in Fig. 3b is shown in Fig. 4c, which concentrates the wider main lobe near the real main lobe, greatly reduces the width of the sidelobes or even eliminates the sidelobes. At the same time, it greatly reduces the values of M and N , and reduces the computational time cost. The m and p values can be as large as possible to improve the accuracy of spectrum recognition.

For the background project, taking the upstream side of the A8 cable of the North Tower as an example, after parameter debugging, excessively large m value will cause the noise side lobe to protrude, excessively large p value will lead to an increase in the calculation time, and too small p will have more noise side lobes and cannot be identified. After trial calculation, when $m = 50$ and $p = 50$, the peak focusing of FSP has a good effect, and the calculation speed is fast, and each main lobe is very obvious in the spectrum, which has a good effect on the extraction of the peak and the calculation of the fundamental frequency. The spectrogram obtained by FSP is shown in Fig. 5.

Select the first five frequencies on the upstream side of North Tower A8 cable as the object of automatic extraction. The calculation of the frequency vector can be determined by a priori based on the vibration characteristics of the structure. According to the APES spectrum, it is preliminarily determined that the fourth-order frequency of the North Tower A8 cable is in the range between 1.58 Hz and 1.88 Hz, and the frequency value exceeding this interval can be regarded to be abnormal cable force. The first five-order frequencies every 20 s are obtained in the entire online spectrum analysis framework, as shown in Fig. 6 below.

3.3 Selection of fundamental frequency

Due to the low installation position of the accelerometer, the fundamental frequency and other low-order peak energies are small, and the frequency difference between

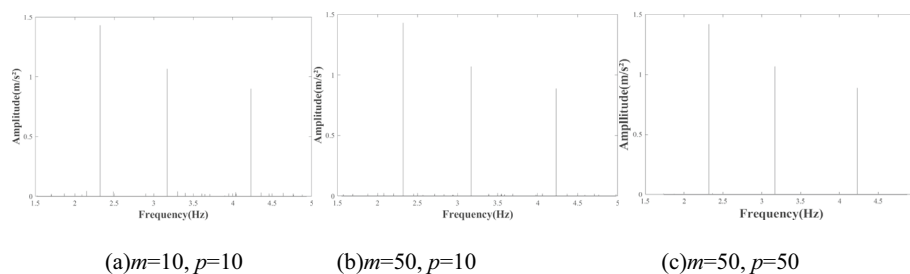


Fig. 4 The aggregation effect of FSP on the spectrum under different m and p values

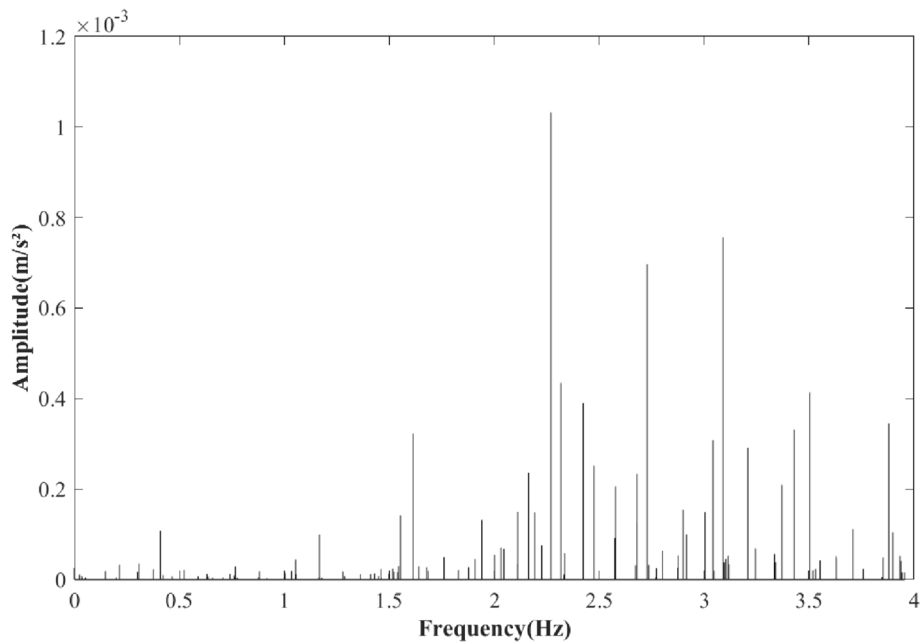


Fig. 5 Spectrogram of FSP on the upstream side of A8 cable

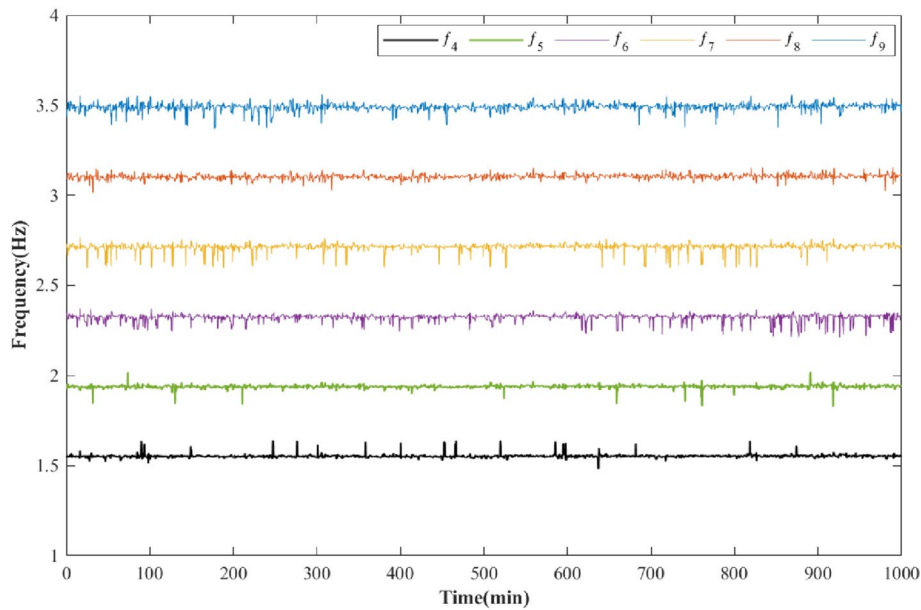


Fig. 6 The first five frequency time periods of the upstream side of the A8 cable in the North Tower

the first-order peak frequency and the high-order peak are large. Therefore, direct detection of the first order frequency may induce large errors. For the traditional average frequency difference method, although part of the errors can be reduced by the averaging calculation, the deviation of any order frequency difference may lead to the deviation of the fundamental frequency calculation results. Moreover, the peak frequency that is difficult to pick up can increase the calculation errors.

According to Ren et al.'s (2005) measurement results, there is a clear multiple relationship between the fundamental frequency and the natural frequency. The fundamental frequency is the natural frequency divided by its corresponding order.

The fundamental frequency method (Timoshenko 1990) can be used to identify the cable frequency under the excitation of a stationary random environment. Due to the difficulty in finding the fundamental frequency of the cable, various high-order resonance peaks are usually used to calculate the fundamental frequency of the bridge cable vibration. Firstly, select the resonant peak with the highest amplitude from the spectrum and record its frequency f_n , which should be the n th natural frequency. Assuming it is a peak formed by the n_1 resonant frequency of cable, then calculate the assumed fundamental frequency $F_1 = f_n/n_1$. According to string vibration theory, the other resonant peaks should be integer multiples of F_1 . Therefore, if the ratio of each resonant peak to the fundamental frequency F_1 is very close to an integer (with a deviation not exceeding ± 0.05), it can be considered as the fundamental frequency F ; Otherwise, add or subtract n_1 and try again until find the fundamental frequency F .

The basic idea of the fundamental frequency method is to search for the frequency f_m corresponding to the highest point of the whole graph, and then determine its corresponding order, from which the fundamental frequency is deduced as f :

$$f = \frac{f_m}{n} \tag{13}$$

Here is an example to illustrate the resistance of the fundamental frequency method to errors caused by small deviations in individual peak frequencies.

Assuming that the natural frequency of a cable is 0.500 Hz, six peaks are detected in its spectrum using the dynamic measurement method, and the fourth peak is the highest peak. Ideally, the corresponding frequencies of each peak are shown in Table 1:

The calculation process of directly reading the fundamental frequency method is shown in Eq. 14:

$$f_d = f_1 = 0.500 \text{ Hz} \tag{14}$$

The calculation process of the average frequency method is shown in Eq. 15:

$$f_a = \frac{(f_2 - f_1) + (f_3 - f_2) + (f_4 - f_3) + (f_5 - f_4) + (f_6 - f_5)}{5} = 0.500 \text{ Hz} \tag{15}$$

The calculation process of the fundamental frequency method is shown in Eqs. 16 and 17:

$$n = \frac{f_m}{f_\Delta} = \frac{2.000}{0.500} = 4 \tag{16}$$

Table 1 Ideal corresponding frequencies of each peak

Peak order	1	2	3	4	5	6
Frequency	0.500Hz	1.000Hz	1.500Hz	2.000Hz	2.500Hz	3.000Hz

$$f = \frac{f_m}{n} = \frac{2.000}{4} = 0.500 \text{ Hz} \tag{17}$$

where $f_{\Delta} = f_a$, the same below.

In reality, due to various factors, the peaks of each order will have a certain deviation. Assuming that the corresponding frequencies of each peak are shown in Table 2 (assuming that the fourth peak is still the highest peak, according to the assumption of the fundamental frequency method, this peak has less deviation compared to the theoretical situation):

The calculation process of directly reading the fundamental frequency method is shown in Eq. 18:

$$f_d = f_1 = 0.600 \text{ Hz} \tag{18}$$

The calculation process of the average frequency method is shown in Eq. 19:

$$f_a = \frac{(f_2 - f_1) + (f_3 - f_2) + (f_4 - f_3) + (f_5 - f_4) + (f_6 - f_5)}{5} = 0.530 \text{ Hz} \tag{19}$$

The calculation process of the fundamental frequency method is shown in Eqs. 20 and 21:

$$n = \frac{f_m}{f_{\Delta}} = \frac{2.050}{0.530} = 3.868 \approx 4 \tag{20}$$

$$f = \frac{f_m}{n} = \frac{2.020}{4} = 0.505 \text{ Hz} \tag{21}$$

The relative errors between the fundamental frequency calculated by three methods and the theoretical values are listed in Table 3.

As can be seen from the results, thanks to the rounding calculation of the fundamental frequency method and the high reliability of the highest peak frequency, the calculation result of the fundamental frequency method is least affected and has the best robustness when the peaks in the spectrum shift. Therefore, the subsequent calculation and analysis will use the fundamental frequency method to identify the natural frequency of the cable.

Table 2 Real corresponding frequencies of each peak

Peak order	1	2	3	4	5	6
Frequency	0.600Hz	1.050Hz	1.500Hz	2.020Hz	2.650Hz	3.250Hz

Table 3 Relative errors of three methods

Method	Result	Theoretical value	Relative error
Directly reading the fundamental frequency method	0.600Hz	0.500 Hz	20%
Average frequency method	0.530Hz	0.500Hz	6%
Fundamental frequency method	0.505Hz	0.500Hz	1%

According to the fundamental frequency method and the automatically extracted frequencies of each order, the fundamental frequency obtained every 20s interval can be automatically extracted. The time-varying fundamental frequency of different cables on the upstream side of the north tower is shown in Fig. 7.

4 Analysis and evaluation of the bridge cable force

4.1 Calculation of cable tension

The tension string theory, which ignores the bending stiffness and sag of the cable, is widely used to obtain the cable-stayed force (Ji et al. 2024). The simplified relationship ignores the influence of cable bending stiffness and sag, which is convenient for rapid engineering application, but may bring unacceptable errors. In response to such a problem, the energy method considers the bending stiffness and sag of the cable. We derive a practical formula for converting cable tension from natural frequency and its applicable range. In this study, the cable force is calculated based on the energy method, with consideration of sag effect and bending stiffness of the cable. Ren et al. (2005) proposed an empirical formula to estimate cable tension considering cable sag effect. By estimating the cable force F_c in advance, the parameter λ^2 characterizing the influence of sag should be in the range between 0.17 and $4\pi^2$. The real bridge cable force F_c is calculated iteratively using Eq. 22:

$$F_c = \sqrt[3]{mL^2(4f^2F_c^2 - 7.569mEA)} \quad (0.17 < \lambda^2 < 4\pi^2) \quad (22)$$

where T is the tension of the cable; m is the mass of the cable per unit length; L is the chord length of the cable; f is the fundamental frequency of the cable; EA is the tensile stiffness; λ is the dimensionless parameter that characterizing the influence of sag, $\lambda^2 = \left(\frac{mgL}{H}\right)^2 \frac{EAL}{HL_e}$; L_e is an integral term, $L_e = \int_0^L \left(\frac{ds}{dx}\right)^3 dx \approx L \left[1 + \frac{1}{8} \left(\frac{mgL}{H}\right)^2\right]$; H is the component of the cable force.

In this formula, the cable force is obtained iteratively. The specific method is as follows: first, assume an initial value, input it into Eq. (22), and calculate the new cable force value. Then, bring the newly obtained tension value back in and continue the operation. Until the difference between the new tension value and the input value is very small, the iteration stops and the true tension is finally obtained.

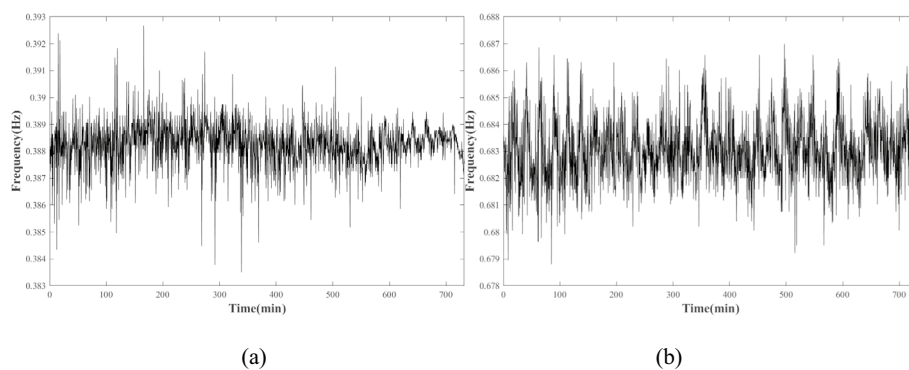


Fig. 7 Diagram of the base frequency time history of the cable (a) cable A8 in the North Tower (b) cable A16 in the North Tower

Since the cable force time history obtained by monitoring has problems such as missing and noise, the moving average method was used to remove the noise, and the median absolute deviation method was used to eliminate the outliers, and the readability of the data was improved through data cleaning. The correctness of the SHM data was verified by combining with the manual inspection data, and abnormal data caused by acceleration sensor failure in the cable force time history data were eliminated. The results of the time history of the cable force are shown in Fig. 8.

4.2 Cable performance evaluation based on the cable force time history

The cables of cable-stayed bridges connect the bridge towers to the main girders and maintain the balance of the entire structure through the transmission of cable forces, providing stability for cable-stayed bridges. Therefore, the magnitude of the cable force of the bridge is crucial to control the deflection and deformation of the bridge. By adjusting the magnitude and distribution of cable force, the deflection and deformation of the bridge can be effectively reduced, and the stiffness and stability of the bridge can be improved (Atmaca et al. 2022). For all cables of a cable-stayed bridge, the closer the tension of each cable is to the design cable force, the better the health condition is of the structure. On the contrary, if there exist cables whose tension is too large or too small relative to the design cable force, then the cable force state of the entire bridge has deviated from the design state, showing that performance degradation may have occurred in the bridge structure. At the same time, the value of the cable force should not exceed the bearing capacity of the cable material.

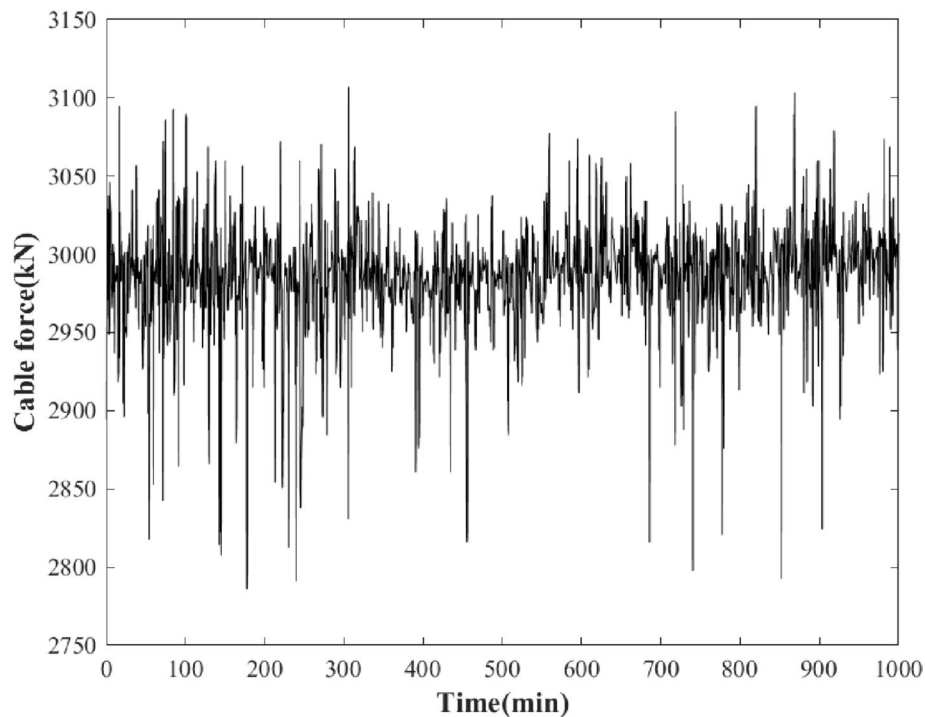


Fig. 8 South Tower J16 cable upstream cable force time history

According to the above analysis, the cable force is taken as the tracking parameter in the damage identification process, and the measured cable force of the undamaged structure and the measured cable force of the damaged structure are taken as the known conditions. The tension of the cables can be considered as a modest indicator model, which means that there is a standard state, and the closer to this standard value, the better. According to this principle, if the measured cable force F_i is equal to the measured cable force F_{i0} of the undamaged structure, the evaluation value x_i can be rated as a full score. If the measured cable force F_i of the damaged structure deviates from the standard state F_{i0} to a certain extent, it will be rated as a zero score. At the same time, it is also necessary to consider whether the cable force is close to the upper limit of the cable material's bearing capacity. When the tensile stress in the cable is close to the strength of the material, it is already extremely unsafe and x_i should also be judged as a zero point.

The degree of deviation of the cable force from the standard state is quantified as a percentage of the change in the cable force, and a certain percentage is used as the zero-point criterion. Considering the moderate index model and the material strength, the cable force deviates from the standard state by 40% as the zero point standard, and the curve is interpolated according to the moderate index model:

$$x_i = f(F_i) = \begin{cases} 100 \left(\frac{F_i - 0.6F_{i0}}{F_{i0} - 0.6F_{i0}} \right) \exp \left[-0.5 \left(\frac{F_i - 0.6F_{i0}}{F_{i0} - 0.6F_{i0}} - 1 \right) \right], & 0.6F_{i0} < F_i < F_{i0} \\ 0, & F_i \leq 0.6F_{i0} \text{ or } F_i \geq 1.4F_{i0} \\ 100 \left(\frac{1.4F_{i0} - F_i}{1.4F_{i0} - F_{i0}} \right) \exp \left[-0.5 \left(\frac{1.4F_{i0} - F_i}{1.4F_{i0} - F_{i0}} - 1 \right) \right], & F_{i0} < F_i < 1.4F_{i0} \end{cases} \quad (23)$$

By determining the condition of the component according to the standard listed in Table 4, the condition corresponding to the structural response can be judged in time and the corresponding maintenance measures can be taken.

According to the above model, for each cable force value, a corresponding rating grade can be obtained. Figure 9 shows the cable score obtained every 20seconds, and the real-time advantage of the SHM system can be used to quickly respond to emergencies. If the force rating grade is 3 or below, a timely decision should be made for maintenance. This real-time monitoring and evaluation method can detect abnormal cable forces or deviations from the design state in time, ensuring the structural safety and health of cable-stayed bridges.

5 Conclusion

In this paper, an APES-based method for cable force extraction is proposed, which is then optimized using FSP. The APES algorithms and cable force assessment index was combined to evaluate the cable performance. In addition, FSP algorithm was used to

Table 4 Cable-stayed force evaluation criteria

Rating Grade	Rating of Cable-stayed Force	Component condition
1	81–100	Excellent
2	61–80	Good
3	41–60	Poor
4	21–40	Extremely poor
5	0–20	Dangerous

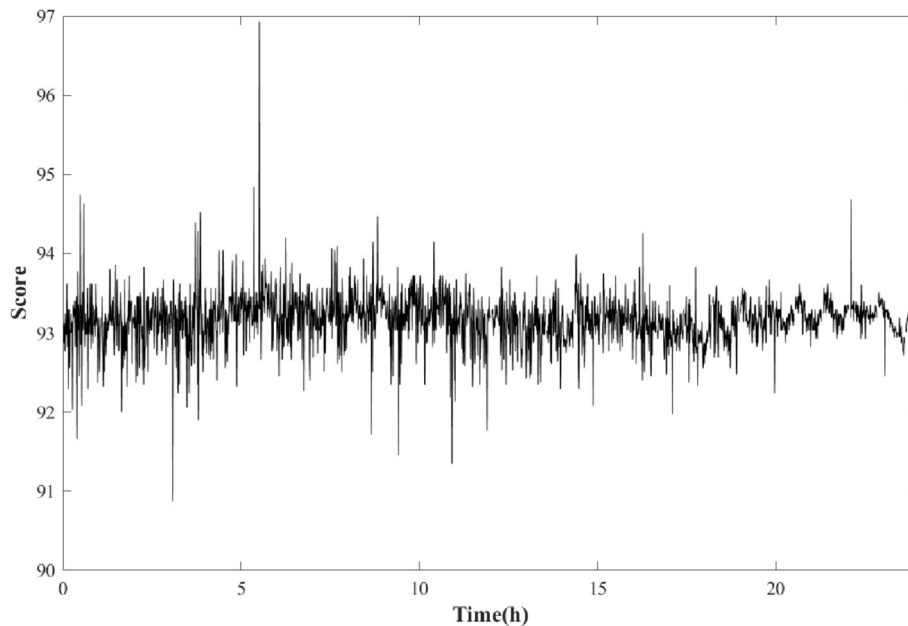


Fig. 9 South tower J8 cable real-time scoring sequence

simplify the spectrum in the process of extracting the fundamental frequency of the cables. The detected cable forces are evaluated according to the interpolation of the moderate index model to realize the real-time assessment of the bridge service performance. The following conclusions can be drawn from this study:

- 1) The time-frequency diagram obtained by the APES algorithm and post-processing method has higher resolution, more concentrated energy, clearer frequency line, more accurate amplitude information, than traditional FFT method. Moreover, the sample data length needed is much smaller than FFT, with lower analysis delay. Compared with the traditional offline processing method, it has faster time-frequency analysis speed.
- 2) Based on the algorithm of automatic extraction of frequency and amplitude, the automatic extraction of peak values of spectrogram is realized. The amplitude can be used to measure the reliability of the recognition frequency, and then used for rapid identification of cable-stayed bridge cable forces.
- 3) The full score and zero score states are defined based on the fixed percentage of cable force change, and the moderate index model for curve interpolation is used. The proposed method can quickly realize the real-time scoring of the cable force to meet the needs of real-time monitoring and evaluation of the SHM system.

Acknowledgements

The authors would like to express their gratitude for the support received.

Authors' contributions

WW performed data analysis and was a major contributor in writing the manuscript. XS contributed to the conception of the study and revised the manuscript. YY conducted the statistical analysis. HC performed data analysis. WY conducted the analytical analysis. WX performed the analysis with constructive discussions. The authors have read and approved the final draft of the manuscript.

Funding

This research was supported by National Natural Science Foundation of China (No. 52378287), the Natural Science Foundation of Jiangsu (No. BK20201274) and Provincial and Ministerial Key Laboratory Scientific Research Project (No.2242023K30017).

Availability of data and material

The datasets used during the current study are available from the corresponding author on reasonable request.

Declarations**Competing interests**

Non-financial competing interests.

Received: 5 February 2024 Accepted: 5 April 2024

Published online: 10 June 2024

References

- Ali K, Katsuchi H, Yamada H (2020) Comparative study on structural redundancy of cable-stayed and extradosed bridges through safety assessment of their stay cables. *Engineering* 7(prepublish):111–123
- Atmaca B, Ghafoori R, Dede T, Ateş Ş (2022) The effect of post-tensioning force and different cable arrangements on the behavior of cable-stayed bridge. *Structures* 44:1824–1843
- Baccigalupi A, Liccardo A (2016) The Huang Hilbert transform for evaluating the instantaneous frequency evolution of transient signals in non-linear systems. *Measurement* 86:1–13
- Cicone A, Liu J, Zhou H (2016) Adaptive local iterative filtering for signal decomposition and instantaneous frequency analysis. *Appl Comput Harmon Anal* 41:384–411
- Hou S, Dong B, Fan J, Wu G, Wang H, Han Y, Zhao X (2021) Variational mode decomposition-based time-varying force identification of stay cables. *Appl Sci-Basel* 11(3):1254
- Ji J, Hung S, Akbar Y, Huang K, Wang R (2024) Node-based wave analysis method for the dynamic response and stiffness of long-span cable-stayed bridges. *Structures* 59105722
- Li J, Stoica P (1996) An adaptive filtering approach to spectral estimation and SAR imaging. *Signal Process* 44(6):1469–1484
- Li S, Wei S, Bao Y, Li H (2018) Condition assessment of cables by pattern recognition of vehicle-induced cable tension ratio. *Eng Struct* 155:1–15
- Ni P, Li J, Hao H, Xia Y, Wang XY, Jae-Myung L, Kwang-Hyo J (2018) Time-varying system identification using variational mode decomposition. *Struct Control Health Monit* 25(6):e2175
- Noel AB, Abdaoui A, Elfouly T, Ahmed MH, Badawy A, Shehata MS (2017) Structural health monitoring using wireless sensor networks: a comprehensive survey. *Commun Surv Tutor* 19(3):1403–1423
- Pai PF (2010) Online tracking of instantaneous frequency and amplitude of dynamical system response. *Mech Syst Signal Process* 24:1007–1024
- Ren W, Chen G, Hu W (2005) Empirical formulas to estimate cable tension by cable fundamental frequency. *Struct Eng Mech* 20(3):363–380
- Timoshenko S (1974) *Vibration problems in engineering*, 4th edn. Wiley
- Xin Y, Li J, Hao H (2021) Enhanced vibration decomposition method based on multisynchrosqueezing transform and analytical mode decomposition. *Struct Control Health Monit* 28:e2730
- Yang Y, Li S, Nagarajaiah S, Li H, Zhou P (2016) Real-time output-only identification of time-varying cable tension from accelerations via complexity pursuit. *J Struct Eng* 142(1):01568473
- Yu X, Dan D (2022) Online frequency and amplitude tracking in structural vibrations under environment using APES spectrum postprocessing and Kalman filtering. *Eng Struct* 259:114175
- Zarraf MAHES, Norouzi M, Allemang R, Hunt V, Helmicki A, Venkatesh C (2018) Vibration-based cable condition assessment: a novel application of neural networks. *Eng Struct* 177:291–305
- Zhang X, Peng J, Cao M, Damjanović D, Ostachowicz W (2020) Identification of instantaneous tension of bridge cables from dynamic responses: STRICT algorithm and applications. *Mech Syst Signal Process* 142:106729
- Zhong R, Pai PF (2021) An instantaneous frequency analysis method of stay cables. *J Low Freq Noise Vib Act Control* 40(1):263–277

Publisher's Note

Springer Nature remains neutral with regard to jurisdictional claims in published maps and institutional affiliations.